Dynamics of Hydrogen Isotope Absorption and Emission of Neutron-Irradiated Tungsten*)

Takeshi TOYAMA[1)], Miyuki YAJIMA[2)], Noriyasu OHNO[3)], Tatsuya KUWABARA[3)], Vladimir Kh. ALIMOV[1,4,5)] and Yuji HATANO[6)]

[1)]*Institute for Materials Research, Tohoku University, Oarai 311-1313, Japan*
[2)]*National Institute for Fusion Science, Toki 509-5292, Japan*
[3)]*Graduate School of Engineering, Nagoya University, Nagoya 464-8063, Japan*
[4)]*National Research Centre "Kurchatov Institute", Moscow 123182, Russia*
[5)]*A.N. Frumkin Institute of Physical Chemistry and Electrochemistry, Russian Academy of Sciences, Moscow 119071, Russia*
[6)]*Hydrogen Isotope Research Center, Organization for Promotion of Research, University of Toyama, Toyama 930-8555, Japan*

(Received 13 March 2020 / Accepted 29 September 2020)

This overview presents recent results regarding hydrogen isotope absorption and emission dynamics in neutron-irradiated tungsten (W) using our recently developed Compact Diverter Plasma Simulator (CDPS), a linear plasma device in a radiation-controlled area. Neutron irradiation to 0.016 - 0.06 displacement per atom resulted in a significant increase in deuterium (D) retention due to trapping effects of radiation-induced defects. We analyzed the dependency of D retention on the D plasma fluence by exposing neutron-irradiated pure W to D plasma at 563 K over a range of D fluence values. The total retention was revealed to be proportional to the square root of D fluence, indicating that the implanted D atoms first occupy the defects caused by neutron-irradiation near the surface and then the defects located in deeper regions. We further investigated the effects of post-plasma annealing on D emission; neutron-irradiated pure W was exposed to D plasma at 573 K and was then annealed at the same temperature for 30 hours. Approximately 10% of the absorbed D was released by annealing, suggesting that a heat treatment of the plasma-facing component of a fusion reactor at moderately elevated temperatures could contribute to the removal of accumulated hydrogen isotopes. The experimental results obtained in this study were only available by investigating neutron-irradiated specimens with the CDPS system, which will be essential for future studies of material behavior and plasma-wall interactions in the fusion reactor environment.

Keywords: tungsten, neutron irradiation, TDS, deuterium

DOI: 10.1585/pfr.15.1505081

1. Introduction

Tungsten (W) is a primary candidate material for plasma-facing components (PFCs) due to its high melting point and high sputtering resistance to energetic particles [1, 2]. The very low solubility of hydrogen isotopes in W is a notable advantage in reducing tritium (T) retention during the operation of fusion reactors [1,3]. However, recent studies have reported that neutron irradiation and ion irradiation cause significant enhancement of hydrogen isotope retention in W [4–7] due to hydrogen trapping at irradiation-induced defects, such as vacancies, vacancy clusters, and dislocation loops [6, 8–10]. Therefore, to improve the prediction accuracy and control over T retention within W in the fusion reactor environment, it is essential to understand the dynamics of hydrogen isotope absorption and desorption in W containing irradiation-induced defects.

Recently, we successfully developed a linear plasma device, the Compact Diverter Plasma Simulator (CDPS), in a radiation-controlled area that can produce steady-state deuterium (D) and/or helium plasma. The CDPS facilitates plasma-wall interaction studies of neutron-irradiated materials [11]. Characteristic features of the CDPS system include the availability of radioactive W samples after neutron irradiation; precise control of the sample temperature before, during, and after plasma exposure; and thermal desorption spectrometry (TDS) measurement without exposing W samples to air following plasma exposure. Thus, the CDPS can be used to improve the reliability of plasma-wall interaction experiments.

To study the dynamics of hydrogen isotope absorption, several studies have proposed transport models of W containing irradiation-induced defects [7, 12, 13]. These models assume that hydrogen diffuses into W by filling

author's e-mail: t.toyama@tohoku.ac.jp
*) This article is based on the invited talk at the 36th JSPF Annual Meeting (2019, Kasugai).

trapping sites from the surface region toward inner regions. Therefore, an interface is expected between the "filled zone", where almost all trapping sites are occupied by hydrogen, and the "empty zone", where most trapping sites remain unoccupied. Such an interface would move away from the surface with increasing hydrogen absorption. These models also predict that hydrogen retention is proportional to the square root of the amount of hydrogen implantation, i.e., plasma exposure time. However, these models remain to be validated, due to a lack of experimental studies examining the kinetics of hydrogen absorption in W containing irradiation-induced defects. Recently, we conducted a study of the kinetics of D absorption in neutron-irradiated W, and explored variation in D retention using D plasma exposure time as a parameter [14]. Hydrogen retention was found to be proportional to the square root of the plasma exposure time, providing the first clear evidence that the proposed transport models are valid.

From the perspective of fusion reactor design and operation, T removal from PFCs after a regular campaign of reactor operation is a critical issue [15]. One promising approach to T removal is heating PFCs in a vacuum after the operation period using the radioisotope decay heat (e.g., ~573 K for 1 month) induced by neutron irradiation. In a pioneering study, we quantitatively measured D emission from neutron-irradiated W samples exposed to D plasma, and found that heating at 573 K contributes to D emission [16].

In this overview, recent results regarding hydrogen isotope absorption and emission dynamics in neutron-irradiated W via the CDPS are introduced, to demonstrate the usefulness of the CDPS. A significant increase in D retention in neutron-irradiated W was found, and the observed kinetics of absorption and emission was well-explained by the model of long-distance diffusion of hydrogen isotope atoms under trapping effects at radiation-induced defects.

2. Experimental Apparatus

For D plasma exposure with the CDPS, we fixed a sample on the sample stage, which was equipped with an air-cooling system. A thermocouple was pressed onto the back of the sample to monitor its temperature. Electron temperature and density in the D plasma were measured using an electrostatic probe located at 10 mm from the sample. D ion flux and incident ion energy were precisely controlled by the bias voltage between the plasma and sample stage. The sample temperature was well controlled before, during, and after plasma exposure. Before the start of plasma exposure, low-density D plasma was generated, and the sample was positively biased at +5 V with respect to the plasma potential, to heat the sample to the target temperature through electron bombardment. After the target temperature had been reached, high-density D plasma was generated, and the sample was negatively biased to initiate D plasma exposure. During plasma exposure, the sample temperature was maintained by adjusting the air-cooling flow. An example of sample temperature control during D plasma exposure is shown in Fig. 1, with a target temperature of 563 K and temperature fluctuation within 5 K. After termination of the plasma exposure, the sample temperature was reduced within 5 minutes by air cooling to below 323 K. The sample was then transferred to a vacuum chamber for TDS measurement without exposure to air. The vacuum chamber was externally heated using an infrared heating device. The transfer procedure and chamber structure were described previously [11, 14].

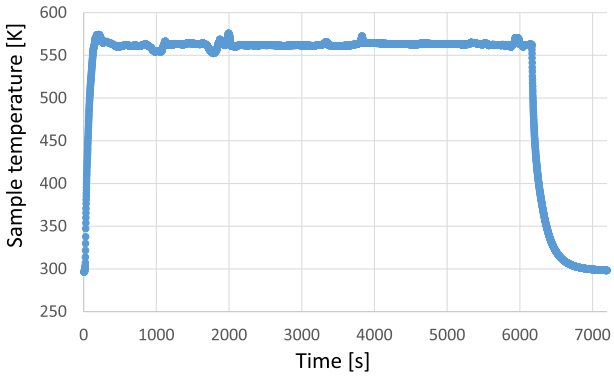

Fig. 1 Example of sample temperature during D plasma exposure.

For TDS measurements, thermocouples were connected to the back of a molybdenum tray. A quadrupole mass spectrometer (MICROVISION-2 100D; MKS Instruments) was used to measure the mass 4 (D_2) signal to determine the D desorption during heating. The mass 4 signal was calibrated using a flow-calibrated leak. The amount of D desorbed as mass 3 (HD) was significantly smaller than that desorbed as D_2.

3. Kinetics of D Absorption and Emission

W samples (99.99 wt. %; A.L.M.T. Corp.) with a diameter of 6 mm and thickness of 0.5 mm were prepared and polished to a mirror-like surface, followed by stress-relief annealing in a vacuum of $\sim 10^{-6}$ Pa at 1173 K for 1 hour. The average positron lifetime of these samples was 117 ps, indicating that there were almost no defects in which positrons could be trapped. Some samples were neutron-irradiated at Belgian Reactor 2 (BR2; SCK/CEN, Belgium) at 563 K to a fluence of 1.1×10^{24} m^{-2} ($E_n >$ 1 MeV), corresponding to 0.06 displacement per atom (dpa). Following neutron irradiation, the samples were electro-polished with a 2-M NaOH solution to remove impurities and oxide layers. The average positron lifetime of the neutron-irradiated samples was 285 ps, which clearly indicated the formation of vacancy-type defects.

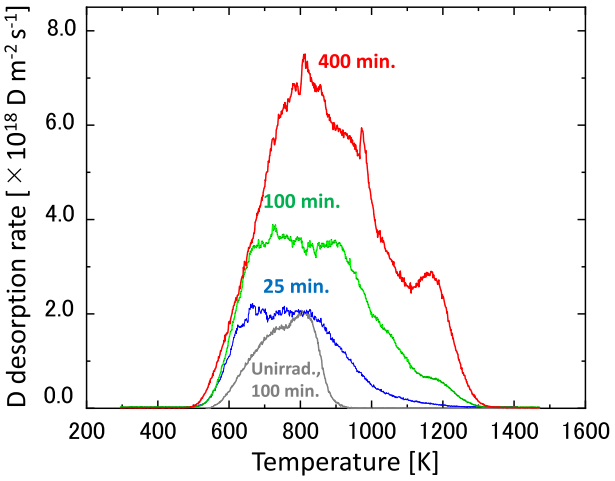

Fig. 2 Thermal desorption profiles of D for W exposed to D plasma at 563 K for 25, 100, and 400 minutes after neutron-irradiation, and that for unirradiated W exposed to D plasma at 563 K for 100 minutes. (Reproduced from Yajima, M. et al., Kinetics of deuterium penetration into neutron-irradiated tungsten under exposure to high flux deuterium plasma, Nucl. Mater. Energy **21**, 100699 (2019), https://doi.org/10.1016/j.nme.2019.100699.)

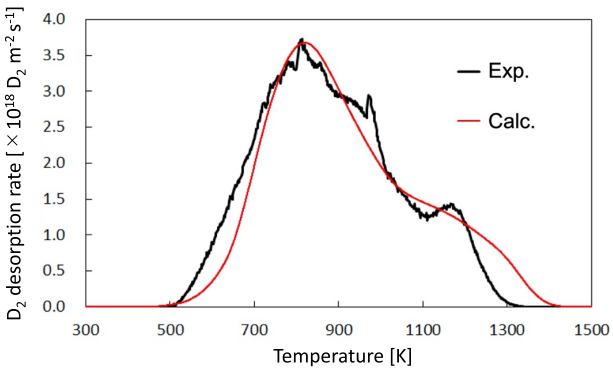

Fig. 3 Thermal desorption profiles of D_2 for W exposed to D plasma at 563 K for 400 minutes after neutron-irradiation (black), and the best fit obtained with TMAP (red). Three types of defects are assumed in the TMAP calculation.

Two-component analysis of the positron lifetime spectrum showed 385 ps for the long component, with ~40% intensity, suggesting vacancy cluster positron trapping as great as $\sim V_{10}$ [17].

Unirradiated and neutron-irradiated samples were exposed to D plasma with an ion flux of 5.4×10^{21} m^{-2} s^{-1}, an incident ion energy of 100 eV, and a sample temperature of 563 K. The plasma exposure time was 100 minutes for the unirradiated sample and 25, 100, or 400 minutes for the neutron-irradiated samples. We also performed plasma exposure at 773 K, for 60 minutes for the unirradiated sample and 15 or 60 minutes for the neutron-irradiated samples.

TDS measurements were performed from room temperature to 1453 K, at an increment of 0.5 K s^{-1}. For each sample, the TDS measurement was started 90 minutes after termination of D plasma exposure.

Figure 2 shows the thermal desorption profiles of D for W exposed to D plasma at 563 K over a certain period of time after neutron-irradiation; the profile for unirradiated W is also shown. For samples exposed for 100 minutes, the total area of the profiles increased significantly after neutron irradiation, indicating that the total D retention also increased. This result is consistent with those of previous studies [4–7, 9]. The amount of D released from the unirradiated sample decreased sharply above 850 K, whereas that released from the neutron-irradiated samples continued to increase at temperatures exceeding 1100 K. Several shoulders/peaks in the curve were observed in these high-temperature regions, suggesting that neutron irradiation induced defects such as dislocations, vacancies, and vacancy clusters, which act as D trapping sites, having a larger binding energy with D than the intrinsic defects. Among the neutron-irradiated samples, the total D retention increased with increasing plasma exposure time.

To examine the D emission dynamics in detail, we analyzed the thermal desorption profiles of D for the neutron-irradiated sample exposed to D plasma for 400 minutes using the Tritium Migration Analysis Program (TMAP) [18]. The detrapping energy and defect concentration of the material were estimated by fitting the experimentally obtained profiles with the thermal desorption profiles.

Because three peaks were observed in the thermal desorption profile for the neutron-irradiated sample exposed to D plasma for 400 minutes (shown in Fig. 2), the first fitting trial was performed using three types of trapping sites. D retention was concentrated in the region near the plasma-exposed surface; therefore, we assumed that no D emission occurred from the rear of the W sample during the first trial. Figure 3 shows the results of the best fit calculation, performed using the following parameters for the three trapping sites: detrapping energies of 1.36, 1.57, and 1.90 eV; and concentrations of 0.12, 0.033, and 0.016 at.%, respectively. Even the best-fit calculated curve tended to broaden in the high-temperature region (> 1000 K). It was difficult to reproduce the profile with a small peak in the high-temperature range. Furthermore, the increase in emission flux at around 600 K was largely underestimated by the calculation.

To evaluate the interactions of multiple defects, we estimated the temporal evolution of the depth distribution of D retention for each defect, as shown in Fig. 4. Before TDS heating (at the sample temperature of 300 K), all three trapping sites were filled with D atoms to a depth of 60 μm. As the sample temperature increased, desorption began from the 1.36 eV-trapping sites. Near the surface, D was released to the outside, and near 60 μm, D diffused into the low-concentration region, such that D retention decreased from both ends of the distribution. When the sample temperature reached 800 K, more than half of the

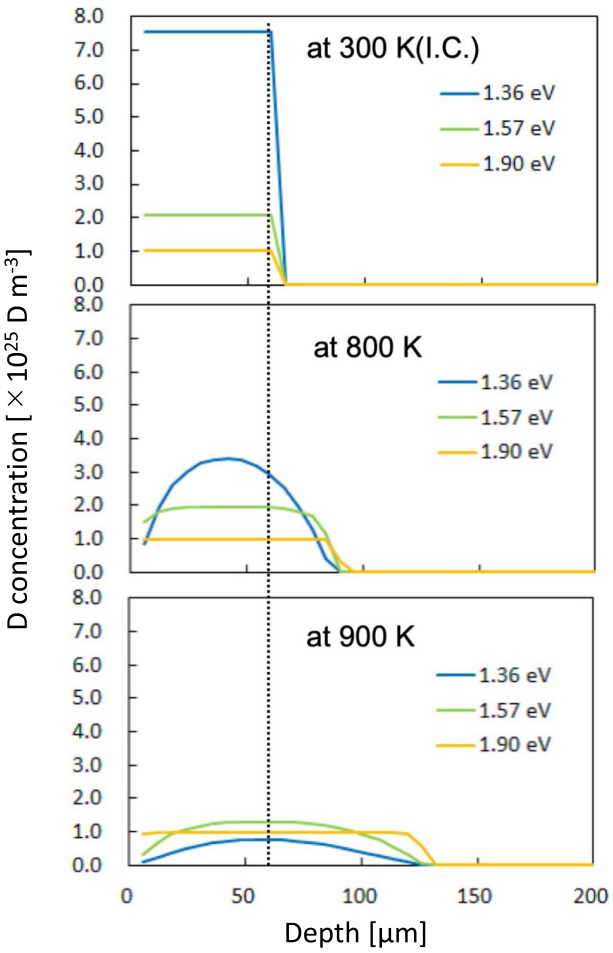

Fig. 4 Depth distribution of D retention with TMAP for W exposed to D plasma at 563 K for 400 minutes after neutron-irradiation. Three types of defects are assumed in the TMAP calculation.

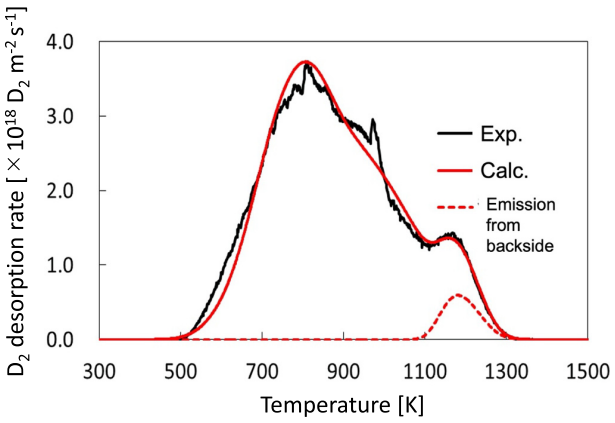

Fig. 5 Thermal desorption profiles of D_2 for W exposed to D plasma at 563 K for 400 minutes after neutron-irradiation (black), and the best fit calculation with TMAP (red). Two types of defects are assumed in the TMAP calculation.

retained D was detrapped from the 1.36 eV-trapping sites. However, D retained at the 1.57- and 1.90-eV trapping sites was distributed throughout the sample, because D that was desorbed from the 1.36-eV trapping sites was captured again by empty trapping sites with high detrapping energy. At higher temperatures, desorption also occurred from the 1.57-eV trapping sites, and the distribution of D retained at the 1.90-eV trapping sites was further expanded. When the sample temperature reached 1100 K, D atoms were hardly captured at the 1.36- and 1.57-eV trapping sites, and desorption occurred from the 1.90-eV trapping sites. At this time point, the distribution of D retained at the 1.90-eV trapping sites reached to ~300 μm. At higher sample temperatures, the distribution became more diffuse, sometimes reaching the rear of the sample. Therefore, it is necessary to consider the release of D from the rear of the sample in the calculation.

Taking the two types of D trapping sites and D emission from the rear surface into account, we calculated the thermal desorption profiles shown in Fig. 5. The detrapping energies of 1.36 and 1.63 eV, and their corresponding trapping site concentrations of 0.16 and 0.044 at.% were assumed. The dashed line indicates the desorption profile from the rear of the sample, and the solid red line indicates the sum of the thermal desorption profiles from the front and rear. We obtained very good agreement for temperatures greater than 1100 K. D emission from the rear of the sample was confirmed by the spread of the distribution, which showed a single independent peak. From the TDS analysis, some of the D atoms desorbed from low-energy trapping sites as the temperature increased were recaptured by high-energy trapping sites within the sample, and the distribution of the retained D was expanded.

Thus, TMAP analysis of the neutron-irradiated sample exposed to D plasma for 400 minutes identified two types of trapping sites with different detrapping energies. D emission from the rear of the sample produced an independent peak in the high-temperature region of the thermal desorption profile.

Figure 6 shows the thermal desorption profiles of D for W exposed to D plasma at 773 K for 15 and 60 minutes after neutron-irradiation, and that for unirradiated W exposed to D plasma at 773 K for 60 minutes. The profile for W exposed to D plasma at 563 K for 25 minutes after neutron-irradiation is also shown as a reference. Negligible D retention was observed in the unirradiated sample; however, in the neutron-irradiated sample, the total D retention increased. The total D retention increased with the plasma exposure time, but was significantly lower than that for plasma exposure at 563 K, perhaps due to enhanced D_2 recombination at the plasma-exposed surface and/or enhanced D release at higher temperatures [19].

Total D retention was given by the total area of the profiles shown in Fig. 2; the result is shown in Fig. 7 as the correlation between plasma exposure time and total D retention. The total D retention was proportional to the

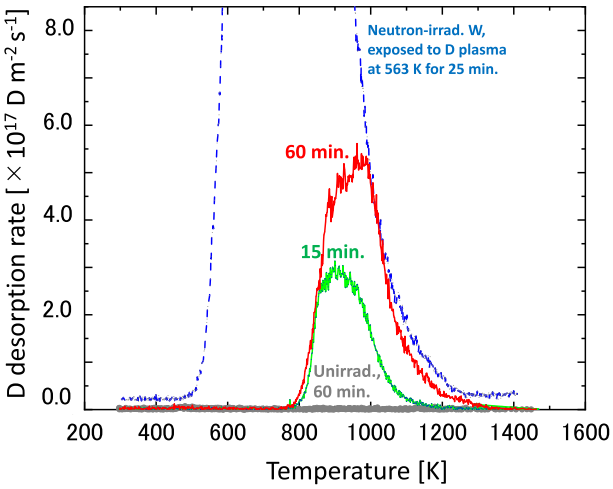

Fig. 6 Thermal desorption profiles of D for W exposed to D plasma at 773 K for 15 and 60 minutes after neutron-irradiation, and that for unirradiated W exposed to D plasma at 773 K for 60 minutes. The profile for W exposed to D plasma at 563 K for 25 minutes after neutron-irradiation is also shown as a reference.

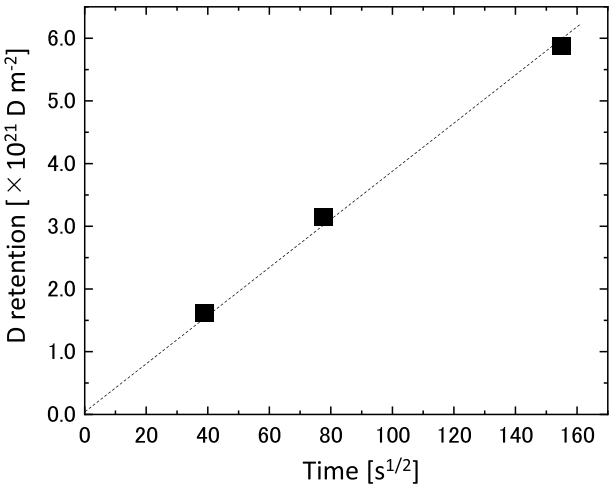

Fig. 7 Correlation between the square root of the plasma exposure time and D retention for W exposed to D plasma at 563 K after neutron-irradiation. (Reproduced from Yajima, M. et al., Kinetics of deuterium penetration into neutron-irradiated tungsten under exposure to high flux deuterium plasma, Nucl. Mater. Energy **21**, 100699 (2019), https://doi.org/10.1016/j.nme.2019.100699.)

square root of exposure time at 563 K. We used TMAP to simulate D diffusion in neutron-irradiated W, assuming a detrapping energy of 1.8 eV and trap density of 0.3 at.% (= 1.9×10^{26} m^{-3}) for neutron-irradiated W [7]. The incident flux was set at 2.7×10^{21} m^{-2} s^{-1} by assuming a reflection coefficient of 0.5. Diffusivity and surface recombination coefficient values were obtained from previous studies [20, 21]. Figure 8 shows the depth profiles of trapped and mobile D for D plasma exposure times of 25 and 100

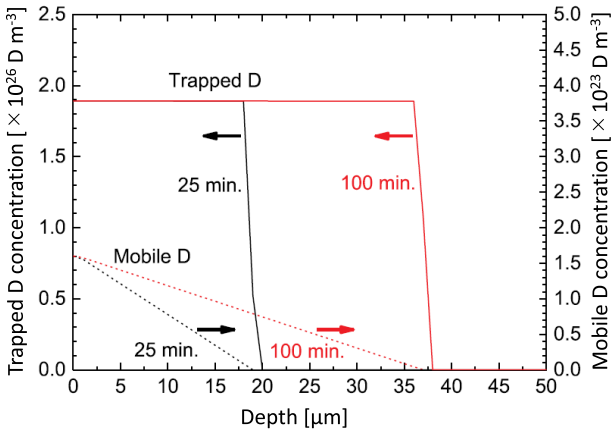

Fig. 8 Depth profiles of trapped D (solid lines) and mobile D (dashed lines) with TMAP for W exposed to D plasma at 563 K for 25 and 100 minutes. (Reproduced from Yajima, M. et al., Kinetics of deuterium penetration into neutron-irradiated tungsten under exposure to high flux deuterium plasma, Nucl. Mater. Energy **21**, 100699 (2019), https://doi.org/10.1016/j.nme.2019.100699.)

minutes. The concentration of trapped D was higher than that of mobile D by orders of magnitude, indicating that D retention was dominated by the amount of trapped D. The concentration of trapped D remained almost constant at 1.9×10^{26} D m^{-3}, reaching 18 and 36 μm at 25 and 100 minutes, respectively, after which it dropped sharply in the deeper regions. There was a clear interface between the near-surface region, where almost all traps were occupied by D (filled zones), and the deeper region, where most trapping sites were empty (empty zone). The depth of this interface increased in proportion to the square root of exposure time, consistent with the data presented in Fig. 7. However, mobile D showed an almost linear concentration gradient from the surface to the interface between the filled and empty zones, demonstrating that the filled zone expanded via D transport driven by the mobile D concentration gradient, as shown in Fig. 8.

Thermal desorption profiles measured after plasma exposure showed a significant increase in D retention following neutron irradiation and continued D release at high temperatures, in contrast to the unirradiated samples. D retention was proportional to the square root of plasma exposure time. These observations support the diffusion model [2], and can be explained by the increase in D penetration depth that occurred with trapping in areas of displacement damage, which created strong D trapping sites. We expect to obtain a more detailed understanding of D penetration kinetics in a future study, which will explore D depth profiling through glow discharge optical emission spectrometry and nuclear reaction analysis.

4. Potential for Hydrogen Isotope Removal by Heat Treatment at Moderately Elevated Temperatures

We used W samples for neutron-irradiated (99.99 wt.%; A.L.M.T. Corp.) and unirradiated reference samples (99.95 wt.%; Goodfellow Cambridge Ltd.), with a diameter of 6 mm and thickness of 0.5 mm. The samples were prepared and polished to a mirror-like surface. Neutron irradiation was performed at BR2, at 563 K to a fluence of 3.0×10^{23} m^{-2} ($E_n > 1$ MeV), which corresponded to 0.016 dpa. After neutron irradiation, the samples were electro-polished with a 2-M NaOH solution.

The unirradiated and neutron-irradiated samples were exposed to D plasma, with an ion flux of 5.4×10^{21} m^{-2} s^{-1} and incident ion energy of ~100 eV at 573 K, for 34 minutes. D cannot fill all neutron irradiation-induced defects throughout the sample under these plasma exposure conditions. Following plasma exposure, some samples were annealed at 573 K for 30 hours. TDS measurements were performed from room temperature to 1453 K, with an increment of 0.5 K s^{-1}.

Figure 9 shows the thermal desorption profiles of D_2 for the unirradiated W samples with and without post-plasma annealing. D retention was observed in the sample without post-plasma annealing. However, almost no D retention was observed in the post-plasma annealing sample, indicating that almost all D was released during post-plasma annealing. Thus, ~99% of total D was released during post-plasma annealing, as has been reported previously [22, 23].

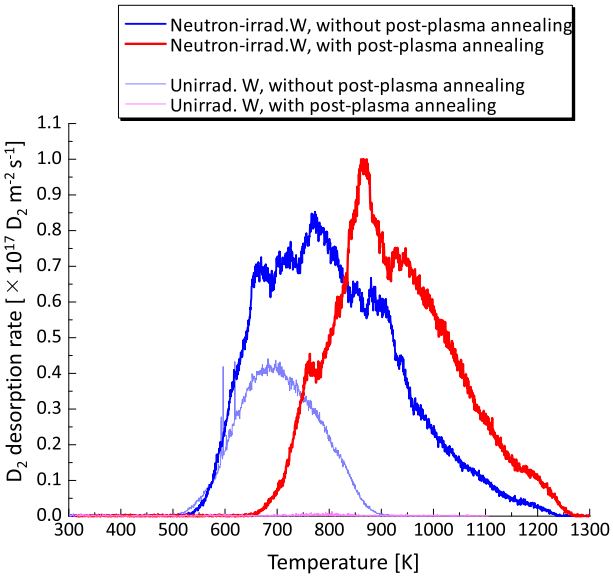

Fig. 9 Thermal desorption profiles of D_2 for W exposed to D plasma at 573 K for 34 minutes after neutron-irradiation and that for unirradiated W exposed to D plasma at 573 K for 34 minutes. Profiles without (purple/blue) and with (pink/red) post-plasma annealing are shown. (Reproduced from Alimov, V. Kh. et al., Deuterium release from deuterium plasma-exposed neutron-irradiated and non-neutron-irradiated tungsten samples during annealing, Nucl. Fusion, **60**, 096025 (2020), https://doi.org/10.1088/1741-4326/aba337.)

Figure 9 also shows the thermal desorption profiles of D_2 for neutron-irradiated W samples with and without post-plasma annealing. The sample without post-plasma annealing showed higher D retention than the unirradiated sample, likely due to D trapping at neutron irradiation-induced defects, as described in Sec. 3. With post-plasma annealing, the total D retention decreased, whereas D release increased at higher temperatures (> 850 K). These findings suggest that some D atoms that had been retained at weak trapping sites were detrapped and released from the sample, whereas other detrapped D atoms were newly trapped at stronger trapping sites. Thus, some detrapped D atoms diffused inward, to be re-trapped in empty traps deeper within the sample during post-plasma annealing. Based on the total area of the thermal desorption profiles, we estimate that ~10% of D was released during post-plasma annealing.

This study is the first to provide experimental data on D desorption during post-plasma annealing. Thus, the heat treatment of PFCs of a fusion reactor at 573 K for 1 month would be an effective method for removing a fraction of T from PFCs; more detailed information is available in [16].

5. Summary

The kinetics of hydrogen isotope absorption and emission were examined by D plasma exposure of neutron-irradiated W under precisely controlled sample temperature and D flux conditions using CDPS and subsequent thermal desorption measurements. Neutron irradiation to 0.016 - 0.06 dpa resulted in significant increase in D retention due to trapping effects of radiation-induced defects. The observed kinetics of absorption and emission was well-explained by the model of long-distance diffusion of hydrogen isotope atoms under the trapping effects.

The absorption process was analyzed by investigating the dependency of D retention on D plasma exposure time. It was found that the D retention is proportional to the square root of the plasma exposure time. This is consistent with the prediction of the diffusion model that neutron-irradiation induced defects near the surface are first occupied with D, after which the defects located in deeper regions become occupied.

The potential for D removal by post-plasma exposure annealing at 573 K was also examined. Approximately 10% of the absorbed D was released during post-plasma annealing at 573 K for 30 hours. This finding suggests that a heat treatment of PFCs in a fusion reactor at 573 K could facilitate the removal of accumulated hydrogen isotopes.

The experimental results obtained in this study were only available by direct comparison between neutron-

irradiated and unirradiated specimens with the CDPS system. Obtaining such results is essential to predict material behavior in the environment inside fusion reactors; thus, world'-leading experimental data on plasma-wall interaction has been obtained. The agreement between the observations and calculations using the diffusion analysis code indicate that this code could be useful for predicting T retention in a fusion reactor when trapping parameters, i.e., trap density, binding energy, etc., are obtained under a wider range of irradiation temperatures and neutron fluences. Further investigations of the behavior of D in neutron-irradiated W with higher neutron fluences is in progress; the results of these studies will further the development of fusion reactor materials.

Acknowledgments

The authors thank Suzuki, K. and Yamazaki, M. for hot laboratory works, and Nagai, Y., Muroga, T. and Masuzaki, S. for their support and encouragement. This work was partially supported by JSPS KAKENHI Grant Number 17H03517 and 18H03688.

[1] Y. Ueda *et al.*, Physica Scripta **T145**, 014029 (2011).
[2] A. Hasegawa *et al.*, Mater. Trans. **54**, 466 (2013).
[3] J. Roth *et al.*, Phys. Scr. **T145**, 014031 (2011).
[4] M. Shimada *et al.*, J. Nucl. Mater. **415**, S667 (2011).
[5] Y. Hatano *et al.*, Mater. Trans. **54**, 437 (2013).
[6] Y. Hatano *et al.*, Nucl. Fusion **53**, 073006 (2013).
[7] Y. Hatano *et al.*, J. Nucl. Mater. **438**, S114 (2013).
[8] K. Ohsawa *et al.*, J. Nucl. Mater. **458**, 187 (2015).
[9] T. Toyama *et al.*, J. Nucl. Mater. **499**, 464 (2018).
[10] K. Ohsawa *et al.*, J. Nucl. Mater. **527**, 151825 (2019).
[11] N. Ohno *et al.*, Plasma Fusion Res. **12**, 1405040 (2017).
[12] W.R. Wampler *et al.*, Nucl. Fusion **49**, 115023 (2009).
[13] D.G. Whyte, J. Nucl. Mater. **390-391**, 911 (2009).
[14] M. Yajima *et al.*, Nucl. Mater. Energy **21**, 100699 (2019).
[15] D. Mueller *et al.*, J. Nucl. Mater. **241-243**, 897 (1997).
[16] V. Kh. Alimov *et al.*, Nucl. Fusion **60**, 096025 (2020).
[17] T. Troev *et al.*, Nucl. Instrum. Meth. B **267**, 535 (2009).
[18] G.R. Longhurst *et al.*, TMAP4 User's Manual, https://doi.org/10.2172/7205576 (1992).
[19] O.V. Ogorodnikova, J. Nucl. Mater. **522**, 74 (2019).
[20] R.A. Anderl *et al.*, Fusion Technol. **21**, 745 (1922).
[21] R. Frauenfelder, J. Vac. Sci. Technol. **6**, 388 (1969).
[22] V. Kh. Alimov *et al.*, J. Nucl. Mater. **417**, 572 (2011).
[23] V. Kh. Alimov *et al.*, J. Nucl. Mater. **420**, 370 (2012).